

Chapter 5

Deadtime and Pileup Correction in the HXDS FPCs and SSDs

Brad Wargelin

5.1 Introduction

The Ortec 671 shaping amplifiers and 921 multi-channel buffers (MCBs) used with the HXDS FPCs and SSDs provide automatic deadtime-correction estimates using built-in circuitry and algorithms that follow the Gedcke-Hale formalism. In most cases, this provides excellent deadtime estimates, particularly for work above several keV using solid state detectors. Our soft x-ray work, however, involves relatively weak signal amplitudes much smaller than such circuitry was designed to work with. In the SSDs, a 2 keV x-ray produces a preamplifier output signal of only 4 mV. The goal with the SSDs was to use them as low as 500 eV, which requires turning down the lower level discriminator (LLD) setting on the MCB to a very low level. At such a low level, the LLD effectively blocks sub-LLD events from appearing in the MCB spectrum, but the cutoff for the electronics processing isn't perfectly sharp and extends to a lower level, where there is a significant amount of steeply rising electronic noise. This hidden noise contamination becomes more severe as the LLD is lowered, and is impossible to avoid at energies below several keV in the SSD. The same problem applies to the FPCs, although less severely because the FPC preamp output signals are about 40 times larger.

The net effect is that sub-LLD, hidden-noise events contribute to the electronic deadtime but are not completely corrected for by the Gedcke-Hale (or any other) built-in deadtime correction circuitry. The alternative is to use the pulser method, in which artificial pulses are injected into the detector preamplifier to mimic real x-ray events. Since the pulses are processed just like x-rays, and subject to the same interactions with hidden noise events, preamplifier reset pulses, etc., the fraction of pulses that appear in the output spectrum is, to a good approximation, equal to the system lifetime. Some care must be taken, however, to make the pulses look something like x-ray signals, avoid under- or over-shoot, and to select a rate as low as possible but high enough to provide adequate statistics.

A pulser cannot perfectly mimic real x-rays because the output pulses are not randomly distributed in time. Most pulsers emit regularly spaced pulses; some are designed to be more random, triggering off electronic noise, but the trigger threshold is continuously adjusted to keep the average pulser rate near the set point, which leads to a pulse distribution which is somewhere between

regular and random. For many applications this is good enough, but not for our system.

A more truly random pulser can be constructed using radioactive decay to trigger a pulse, but there is still a limit to how close together the pulser can emit pulses. Such systems are also more complicated—typically consisting of a radioactive source, a detector, preamplifier, amplifier, single- or multi-channel analyzer, and the pulser which is triggered by a TTL signal from the analyzer—and we didn't have enough rack space or electronic units to use in the 5 pulser systems at XRCF. The XRCF safety officers would also be unenthusiastic about having 5 radioactive sources floating around. We therefore settled on using the regular pulser method, and developed models to correct for the nonrandomness of the pulses.

Historical note: During AXAF calibration at the XRCF, electronic noise was extremely low and we probably could have gotten away with the built-in deadtime estimates for the FPCs. The pulser method, however, was necessary for other work, particularly early on. The HXDS lab originally had a great deal of electronic noise, MCB deadtime errors were very apparent, and something had to be done. Noise was also often a problem when calibrating the detectors at the BESSY synchrotron. Lastly, because of their greater intrinsic noise, the SSDs required pulsers even at XRCF.

5.2 Deadtime and Pileup Time Windows

The time intervals of relevance to our signal processing model are:

T_{shape}	the shaping amplifier time constant
T_{pile}	pileup time window
T_{peak}	time for the shaping amplifier output signal to reach its peak, roughly $2 \times T_{shape}$
T_{width}	full width of the shaping amp output signal, roughly $8 \times T_{shape}$
t	time between one event and the next event.

Treatment of each pulse depends on how closely it is followed by the next pulse:

$0 < t < T_{pile}$	The pileup rejection (PUR) circuitry cannot distinguish between the two events and they are treated as one valid event, with an amplitude equal to the sum of the two.
$T_{pile} < t < T_{peak}$	PUR is activated, and both events are thrown out because the amplitude of neither can be determined
$T_{peak} < t < T_{width}$	PUR is activated, and the second event is discarded
$T_{width} < t$	Both events are processed as valid

The two time windows that really matter are T_{pile} and T_{dead} . $T_{dead} = T_{peak} + T_{width}$ ($-T_{pile}$ if you want to be picky). Notice that T_{peak} is effectively counted twice in T_{dead} (since it is contained within T_{width}), because if the two events occur within that time they are both discarded. Typical times for the shaping time constants we use are:

T_{shape} (μs)	T_{pile} (μs)	T_{dead} (μs)	Detector
0.5	0.6	5.8	(all FPCs used 0.5 μs)
2	0.6	18	(a very few SSD runs used this at XRCF)
10	0.6	75	(almost all the SSD measurements used this)

The table below illustrates the contributions of deadtime and pileup:

T_{shape} (μ s)	X-ray rate (cts/s)	Deadtime (%)	Pileup (%)
0.5	10000	5.64	0.60
0.5	1000	0.58	0.06
10	1000	7.23	0.06
10	100	0.75	0.01

The exact values of T_{dead} and T_{pile} depend on the particular shaping amplifier used (and to a much lesser extent the MCB and preamp). The pileup time, in particular, shows the most relative variation from one unit to another—0.3 to 1.0 μ s. When the pileup rejection is working, pileup events only occur when the two signals peak nearly simultaneously (within T_{pile}), so there is a single pileup peak (assuming a monochromatic input spectrum). When PUR is not working, the second event can ride on the tail of the first, and the MCB will record an event any time a local maximum in the (summed) signal is detected, thus causing lots of “interpeak” events in the spectrum. As was discovered after XRCF, and discussed in Chapter 4, because the SSD preamp signals are so small at low x-ray energies, the pileup rejection starts to fail at about 2 keV. Below that, there is either a partial or complete lack of pileup rejection and deadtime. Approximate corrections for the lack of PUR below 2 keV are explained in Chapter 11.

5.3 Calibration Measurements

Two kinds of measurements were made to calibrate the pulser method: 1) deadtime consistency (DTC) tests, looking at a fixed intensity source with a stable-QE detector under a variety of operational parameters, and comparing the regular pulser method with the radioactively triggered random pulser method, and 2) counting rate linearity (CRL) measurements at the BESSY synchrotron, in which relative incident x-ray rates are known with high precision.

The BESSY CRL measurements were conducted on both SSDs and two FPCs in late 1997 and early 1998, but the data have not yet been analyzed. Relative beam intensity uncertainties are $\pm 0.6\%$ on the SX700 monochromator beamline and $\pm 0.2\%$ on the white beam. For the FPCs, the range of calibrated counting rates was 1000-25000 Hz, with x-ray and pulser statistics of $\pm 0.1\%$. Analysis of the BESSY CRL data may be complicated by the non-random nature of the synchrotron emission—only about half of the ring “buckets” are filled, contiguously.

The DTC testing was conducted in the HXDS lab using a strong radioactive source (^{55}Fe , emitting Mn $K\alpha$ photons at 5.9 keV) and an SSD (ssd_5). FPCs could not be tested with the desired accuracy because their QE is very sensitive to temperature and gas density fluctuations at that energy (we wanted to make measurements to 0.1% accuracy), and because a suitable test chamber was not available in time. FPC testing was also deemed unnecessary because the SSDs and FPCs use identical pulse height analysis electronics chains.

5.4 Deadtime consistency testing

5.4.1 Experimental configuration

DTC tests were conducted Jan. 4–5 1996 and Sept. 18–23 1997 by Brad Wargelin and Mike McDermott. The 1997 data have not been analyzed, but all data were collected in the same way. In the 1996 testing, three types of pulser were used:

- a regular pulser with a fixed rate,
- a (pseudo)random pulser with varying time intervals between pulses and a roughly fixed average rate (triggered by noise),

- and a random pulser which was triggered by radioactive decays,

along with many different combinations of:

- shaping amp time constant (2 or 10 μ s—also 0.5 for the 1997 runs)
- multi-channel buffer lower level discriminator (LLD) setting (20 or 45)
- pulser rate (100 to 500 Hz—30 to 500 Hz for 1997 runs).

Spectra were collected with the x-ray source at two distances from the detector, at x-ray rates of approximately 2900 and 8800 Hz (the highest rate achievable). The 8800-Hz measurements only used a shaping time constant of 2 μ s because the deadtime fraction using the 10- μ s setting would be much too large. Two “random” and two “regular” spectra were collected at the higher x-ray rate, and five random and eight regular spectra at the lower rate. Data using the pseudorandom pulser were problematic to analyze because of the not-regular yet not-really-random nature of the pulses. The results were poor and are not discussed further. Information for the 1996 measurements is tabulated below.

RunID	Approx. R_{x-ray} (cts/s)	LLD	Approx. R_{pulser} (cts/s)	T_{shape} (μ s)	Mode	MCB deadtime MCBdead	T_{real} (s)	X-ray counts
80208	8800	20	500	2	random	18.17	300	2210106
80213	8800	20	100	2	random	16.97	1000	7491697
80212	8800	20	500	2	regular	18.39	300	2234150
80217	8800	20	100	2	regular	17.02	1000	7488795
80229	2900	20	100	10	random	21.56	1000	2303596
80230	2900	20	100	2	random	8.50	1000	2765301
80231	2900	20	500	2	random	10.19	1000	2752915
80243	2900	45	200	2	random	4.95	1000	2766311
80244	2900	45	200	10	random	20.73	1000	2318810
80223	2900	20	100	10	regular	21.51	1000	2304904
80224	2900	20	100	2	regular	8.46	1000	2770243
80235	2900	20	500	2	regular	10.05	1000	2749523
80236	2900	20	500	10	regular	24.39	1000	2243354
80237	2900	45	500	10	regular	22.33	1000	2274635
80238	2900	45	500	2	regular	5.41	1000	2758089
80239	2900	45	100	2	regular	4.79	1000	2771131
80240	2900	45	100	10	regular	20.19	1000	2339508

5.4.2 Data reduction

Each spectrum was analyzed by first determining the number of counts in various features:

- N_x – the main x-ray peak (down to 2.5 keV to include the bulk of the shelf)
- N_{xx}^{pile} – the x-ray/x-ray pileup peak
- N_p – the pulser peak
- N_{xp}^{pile} – the x-ray/pulser pileup peak.

The number of injected pulses (N_{pin}) and the total exposure time (T_{real}) were also recorded for each measurement.

Note that it was not necessary to fit the x-ray peaks, since we were only interested in whether or not we got the same rate when looking at the same signal. Regions of interest (ROIs) were fine to

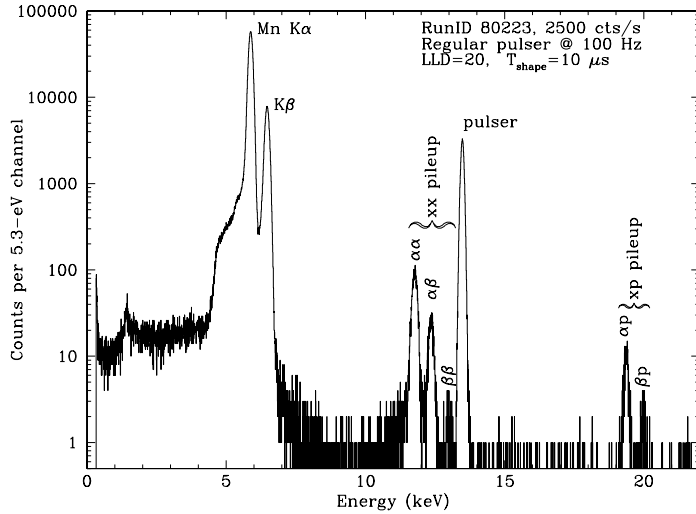


Figure 5.1: Example ^{55}Fe spectrum used in CRL calibration. X-ray and pulser peaks, and resulting pileup, are marked. True x-ray input rate was determined to be 2937.3 ± 5.1 cts/s, with a deadtime of 21.14% and pileup fraction of 0.23%.

use (in fact, more accurate than fitting peaks) because the ^{55}Fe spectrum was so clean, with well-defined features (see Figure 5.1). For consistency, ROIs were adjusted slightly to account for slightly differing energy scales when using different shaping time constants. Errors in N_x determinations are estimated to be less than 0.02%.

Background spectra were also collected for each combination of shaping time constant and LLD setting. Even when nothing appeared in the spectra but the pulser peak (not even electronic noise), the deadtime sometimes exceeded 0.2%. In order to reach our goal of 0.1% measurement accuracy, we therefore assigned a rate of “hidden” events (from sub-LLD noise, discussed above) for each shaping time/LLD combination. The rates R_{hid} were determined from *lifetime fraction* $= N_p/N_{pin} = e^{-(R_{hid}+R_{pin})T_{dead}}$ using equations derived in §5.4.3 and are listed below.

T_{shape} (μs)	LLD	R_{hid} (cts/s)
2	20	150
2	45	20
10	20	10
10	45	0

5.4.3 Correction equations

Corrections were then made to reconstruct what the spectra would look like if 1) pulser events were perfectly random and 2) if there were no pileup. Our corrections are extensions of those described by Bolotin, Strauss, and McClure (NIM 83, 1-12 [1970]). The objective is to derive corrected values for N_x and N_p . T_{dead} and T_{pile} are also determined during the analysis. Once corrected,

pileup and x-ray events experience the same deadtime, and the ratios of corrected detected and input x-ray and pulser events must be same. The input rate of x-ray events is then given by

$$R_{xin} = (N'_x/T_{real})(N'_p/N_{pin}), \quad (5.1)$$

where the prime (') denotes corrected values.

By definition, the system livetime fraction is

$$\begin{aligned} N'_p/N_{pin} &= \text{Probability of 0 events within } T_{dead} \\ &= e^{-(\text{input rate of all events})T_{dead}} \\ &= e^{-(R_{xin}+R_{hid}+R_{pin})T_{dead}}, \end{aligned} \quad (5.2)$$

where we have also used Poissonian statistics, in which the probability of N events occurring within a time interval T when the average rate of the events is R is given by

$$P(R | N, T) = \frac{(RT)^N}{N!} e^{-RT}. \quad (5.3)$$

The value of T_{dead} can thus be determined from

$$T_{dead} = -\ln\left(\frac{N'_p}{N_{pin}}\right)/(R_{xin} + R_{hid} + R_{pin}). \quad (5.4)$$

Likewise the x-ray/x-ray pileup fraction is given by

$$\begin{aligned} N_{xx}^{pile}/N_x &= \text{Probability of 1 x-ray event within } T_{pile} \\ &= R_{xin}T_{pile}e^{-R_{xin}T_{pile}}. \end{aligned} \quad (5.5)$$

The exponential term is nearly 1, and T_{pile} can be adequately approximated as

$$T_{pile} = (N_{xx}^{pile}/N_x)/R_{xin}. \quad (5.6)$$

T_{dead} is used extensively in the equations that follow; T_{pile} is only needed when analyzing non-monochromatic spectra, in which case the number of pileup events, N_{xx} and N_{xp} , usually can not be measured directly and must be estimated.

To correct for pileup, the number of main peak x-ray counts is increased by $2 \times$ number of *xx* pileup counts plus $1 \times$ number of *xp* pileup counts, and the number of main pileup peak counts is increased by $1 \times$ number of *xp* pileup counts. The equations are

$$N'_x = N_x + 2N_{xx}^{pile} + N_{xp}^{pile} \quad (5.7)$$

and

$$N'_p = N_p + N_{xp}^{pile}, \quad (5.8)$$

where the prime (') refers to the corrected number of x-ray or pulser counts (in the absence of pileup).

The nonrandomness corrections are somewhat more complicated, and based on the fact that pulser events cannot interact with themselves the same way they would if they occurred randomly in time. There are therefore fewer (or no) deadtime losses or pileup events, which means that more pulser counts appear in the spectrum than should. Likewise, those “extra” pulser events can interact with x-ray events and lead to the loss of some x-ray counts.

For the regular pulser, pulser events can never cause deadtime for another pulser event because the pulses are too far apart. For the random pulser, pulser events can occur as close together as $2.5 \mu\text{s}$ (limited by the amplifier used to trigger the pulser), which is nearly random but still a non-negligible interval of time. Treatment of the two sets of data is therefore slightly different. Specifically, Eqs. 5.9 and 5.10 are correct only for the regular pulser; the first two occurrences (of three) of “ T_{dead} ” within each must be replaced by “ $2.5 \mu\text{s} - T_{pile}$ ” when the random pulser is used.

Referring to Eq. 5.3, the number of pulser-pulser deadtime events that did not occur, but would have occurred if the pulser were perfectly random is

$$\begin{aligned} N_{pp} &= (\text{Number of input pulses}) \\ &\times (\text{Probability that another pulser event occurs within the deadtime time window}) \\ &\times (\text{Probability that no other non-pulser (x-ray or hidden) events occur during } T_{dead}) \\ &= (N_{pin})(R_{pin}T_{dead}e^{-R_{pin}T_{dead}})(e^{-(R_{xin}+R_{hid})T_{dead}}). \end{aligned} \quad (5.9)$$

Likewise, the number of pulser-pulser-pulser deadtime events that did not occur, but would have appeared in the spectrum if the pulser were perfectly random is

$$\begin{aligned} N_{ppp} &= (\text{Number of input pulses}) \\ &\times (\text{Prob that 2 pulser events occur within the deadtime window}) \\ &\times (\text{Prob that no other non-pulser events occur during } T_{dead}) \\ &= (N_{pin})\left(\frac{(R_{pin}T_{dead})^2}{2!}e^{-R_{pin}T_{dead}}\right)(e^{-(R_{xin}+R_{hid})T_{dead}}). \end{aligned} \quad (5.10)$$

The total number of extra pulser events floating around and able to interfere with non-pulser events is then (excluding negligible higher-order terms)

$$N_{p\ extra} = N_{pp} + 2N_{ppp}. \quad (5.11)$$

Of those extra events, a fraction (about equal to the system livetime) end up in the pulser peak, and the rest (the deadtime fraction) follow an x-ray or hidden noise event within the T_{dead} time window and are discarded. Likewise, some of the extra pulser events create deadtime and cause some x-ray events that should have been recorded to instead be discarded. The number of pulser and x-ray counts must therefore be adjusted as follows:

$$\text{Pulser counts to subtract} = N_{p\ extra}e^{-(R_{xin}+R_{hid})T_{dead}} \quad (5.12)$$

$$\text{X-ray counts to add} = N_{p\ extra}(1 - e^{-R_{xin}T_{dead}}) \quad (5.13)$$

There are higher-order corrections such as the absence of pulser-pulser pileup, and other subtleties such as SSD preamp resets, but they are all negligible and in some cases difficult to accurately quantify, and are not discussed further. The final equations for the pileup- and nonrandomness-corrected numbers of x-ray and pulser counts are therefore

$$N'_p = N_p + N_{xp}^{pile} - (N_{pp} + 2N_{ppp})e^{-(R_{xin}+R_{hid})T_{dead}} \quad (5.14)$$

and

$$N'_x = N_x + 2N_{xx}^{pile} + N_{xp}^{pile} + (N_{pp} + 2N_{ppp})e^{-R_{xin}T_{dead}}. \quad (5.15)$$

Eqs. 1, 4, 9, 10, 14, and 15 are then solved iteratively, using improved values for R_{xin} and T_{dead} until convergence.

Analysis of spectra using the random pulser (which, as noted above, is not completely random since pulses cannot be injected less than $2.5 \mu\text{s}$ apart) is more reliable than when using the regular pulser because the corrections for nonrandomness are smaller. We therefore assume that the x-ray rates derived from the corrected random pulser data are the true rates. The 2.7-year half-life of the ^{55}Fe source was accounted for, leading to rate adjustments of up to 0.07%.

The statistical accuracy of the pulser livetime determination is set by the number of pulses that are lost to deadtime. The fractional error is given by

$$\frac{\sigma_{LT}}{LT} = \frac{[(N_{pin} - N_p)^{0.5}/N_{pin}]}{[N_p/N_{pin}]}. \quad (5.16)$$

Net error is given by quadrature summing of the relative statistical errors in the deadtime and number of x-ray counts.

5.4.4 Results

Using the corrections described above, the following results were obtained:

<hr/>		
random:		
average of 5 tests	2942.8	Hz
average statistical uncertainty (+/-)	3.2	(0.11%)
variance	3.3	(0.11%)
<hr/>		
regular:		
average of 8 tests	2940.2	
average statistical uncertainty (+/-)	3.2	(0.11%)
variance	4.4	(0.15%)
difference from average random result	-2.6	(-0.09%)
<hr/>		
random:		
average of 2 tests	8787.4	
average statistical uncertainty (+/-)	11.4	(0.13%)
variance	4.2	(0.05%)
<hr/>		
regular:		
average of 2 tests	8740.4	
average statistical uncertainty (+/-)	10.9	(0.13%)
variance	1.7	(0.02%)
difference from average random result	-46.6	(-0.53%)
<hr/>		

As can be seen, agreement between the regular- and random-pulser results for the 2900-Hz measurements is excellent. For comparison, the built-in MCB livetime differed from the pulser-method value in some cases by more than 4%. Agreement among the 8800-Hz measurements is not quite as good, but those measurements were made under extreme conditions, far more difficult than any encountered during AXAF calibration. The actual conditions at XRCF (LLD/noise level, pulser rate, and x-ray rate) were much less challenging than in any of our testing.

5.4.5 Simplified and More General Method for Deadtime Determination

The above results were derived for the case of a nearly pure monochromatic source, in which pileup peaks can be easily discerned. For the vast majority of AXAF calibration data, however, it

is difficult to distinguish pileup peaks from continuum spectra, and so a second deadtime-correction program was also written with the intention that it be applied to any spectrum in which one x-ray energy was quasi-dominant, such as in EIPS spectra. That program does not require the number of pileup counts to be determined; those were calculated based simply on the number of (fitted) counts in the x-ray peak, the estimated value of T_{pile} , and the number of pulser peak counts (plus other quantities that are simply read in from the data file header such as integration time T_{real} (`trueTime_sec`) and the number of injected pulses N_{pin} (`autoDeadTime_pulses`).

As a test of its accuracy, this program was used to analyze the regular pulser data described above. Using a fixed value of $0.78 \mu\text{s}$ for T_{pile} (which must be independently determined for each shaping amplifier) the results were:

average of 8 tests	2940.2	Hz
average statistical uncertainty (+/-)	3.2	(0.11%)
variance	4.9	(0.17%)
difference from average random result	-2.6	(-0.09%)
average of 2 tests	8761.7	
average statistical uncertainty (+/-)	11.0	(0.13%)
variance	0.0	(0.00%)
difference from average random result	-25.7	(-0.29%)

At the lower rate, the results were statistically identical. At the higher rate, agreement with the random pulser results improved from 0.5% to 0.3%. This fortuitous improvement was mostly because of a discrepancy in the number of x-ray/pulser pileup counts; the number of observed counts is about 20% larger than predicted. At this time (Mar 1998) the cause of this discrepancy is not known for certain. In any case, the second deadtime correction method works at least as well and is easier.

5.4.6 Estimated accuracy in analysis of AXAF calibration data

The SSD calibration data were taken under more challenging conditions (with respect to deadtime correction accuracy) than for virtually all AXAF calibration data. In particular, the deadtime caused by the pulser (which scales as the product of the shaping time constant and pulser rate) was much higher than used during AXAF calibration, resulting in larger correction terms and therefore larger uncertainties in the final deadtime calculation.

A comparison of the magnitude of deadtime corrections—for the deadtime calibration measurements described above vs. AXAF calibration measurements—was made using model SSD and FPC spectra as inputs, with pulser rates and shaping time constants set to the values actually used during AXAF calibration, specifically:

$$\begin{aligned} \text{SSD shaping time constant} &= 10 \mu\text{s} & \text{pulser rate} &= 27 \text{ Hz} \\ \text{FPC shaping time constant} &= 0.5 \mu\text{s} & \text{pulser rate} &= 300 \text{ Hz} \end{aligned}$$

The two contributions to deadtime correction (pileup and pulser nonrandomness) were calculated, along with the net deadtime correction which may differ slightly from the sum of the two estimated contributions because of the iterative process involved and because the two effects are not entirely independent. In the table of results below, "Raw rate" refers to the x-ray rate derived from uncorrected pulser counts, or

$$\text{Raw rate} = (N_x/T_{real})(N_p/N_{pin}). \quad (5.17)$$

Raw rate(Hz)	Pileup (%)	Pileup corr(%)	Nonrandom corr(%)	Net corr(%)	Final rate
SSD CRL calibration data					
8694.14	1.177	0.076	0.723	0.778	8761.74
8747.94	1.183	0.014	0.151	0.158	8761.72
2919.57	0.361	0.016	0.652	0.668	2939.08
2938.60	0.434	0.016	0.180	0.188	2944.14
2913.85	0.431	0.078	0.791	0.909	2940.34
2848.27	0.352	0.080	3.210	3.404	2945.22
2840.16	0.357	0.080	3.027	3.233	2931.97
2917.14	0.432	0.078	0.795	0.916	2943.87
2928.77	0.434	0.016	0.174	0.181	2934.09
2924.24	0.367	0.015	0.611	0.626	2942.55
Model SSD data					
100.00	0.015	0.004	0.153	0.188	100.19
500.00	0.075	0.004	0.190	0.199	501.00
900.00	0.131	0.004	0.191	0.196	901.78
1200.00	0.170	0.004	0.189	0.193	1202.30
1500.00	0.208	0.004	0.187	0.191	1502.86
Model FPC data					
1000.00	0.155	0.047	0.132	0.172	1001.72
5000.00	0.763	0.046	0.158	0.170	5008.52
10000.00	1.493	0.043	0.158	0.167	10016.70
15000.00	2.191	0.039	0.153	0.161	15024.20
20000.00	2.857	0.034	0.145	0.151	20030.27

Note that the net pileup correction is quite small. This is because the fractions of pileup events added to the main x-ray and pulser peaks are nearly the same (both scaling nearly linearly with x-ray rate), and so the corrections to each roughly cancel out. Also note that the net corrections to the x-ray rates are nearly constant regardless of the rate.

5.5 Recommendations

For SSD spectra at energies above 2 keV, the pulser method must be used since the MCB deadtime estimate can be off by several percent. For the FPCs, the pulser method can always be used, but the MCB deadtime estimate is probably good enough that it can be used *if* pileup corrections are made.

When using the pulser method, whether for SSDs or FPCs:

1. Fit the number of x-ray line counts in the main peak
2. Determine the number of pulser counts (excluding any piled-up counts)
3. $R_{xin} = 1.0018(N_x/T_{real})(N_p/N_{pin})$.

The resulting number, with appropriate statistical uncertainty estimates, should have systematic errors of less than +/-0.10% for rates up to 2500 Hz. For higher rates with the FPCs, systematic errors are estimated to be less than 0.25% at 10000 Hz and 0.50% at 20000 Hz. Note that corrections for pileup are automatically included.

For the FPCs, if you don't want to bother finding the number of counts in the pulser peak, it's probably good enough to use the MCB deadtime. You must correct for x-ray/x-ray pileup,

however, by adding twice the rate of pileup counts back in to the main x-ray peak. Rather than try to fit the pileup peak (which is quite broad in the FPCs, and sits on top of continuum), it's much easier to simply estimate the rate of pileup counts as $R_{pile} = R_{xin} \times T_{pile}$ where T_{pile} is about $0.6 \mu s$. (T_{pile} can be off by +/- $0.2 \mu s$ or so, but that's only a 0.4% error in the x-ray rate at 10000 Hz. Eventually we will analyze selected data from each FPC and SSD to determine T_{pile} for each shaping amp.)

To make sure you handle the pileup correction correctly, with the proper deadtime, use this equation:

$$R_{xin} = N_x / T_{live} [1 + 2T_{pile} N_x / T_{live}] \quad (5.18)$$

where T_{live} is the MCB livetime listed in the *.pha file header (`liveTime_sec`).

5.6 Appendices

Two FORTRAN programs were used to derive the results presented above. `do98_12.f` is for analyzing the SSD deadtime consistency data. `test.data` is the input file and `do98_12.out` is the output file. `correct4.f` can be used to analyze the results from any spectrum, and calculates the expected xx and xp pileup so that those peaks don't have to be fitted in the spectrum. Sample input and output files are also listed. Files are located at <http://hea-www.harvard.edu/MST/hxds/topics/> under "Deadtime and Pileup Correction in the HXDS FPCs and SSDs."